#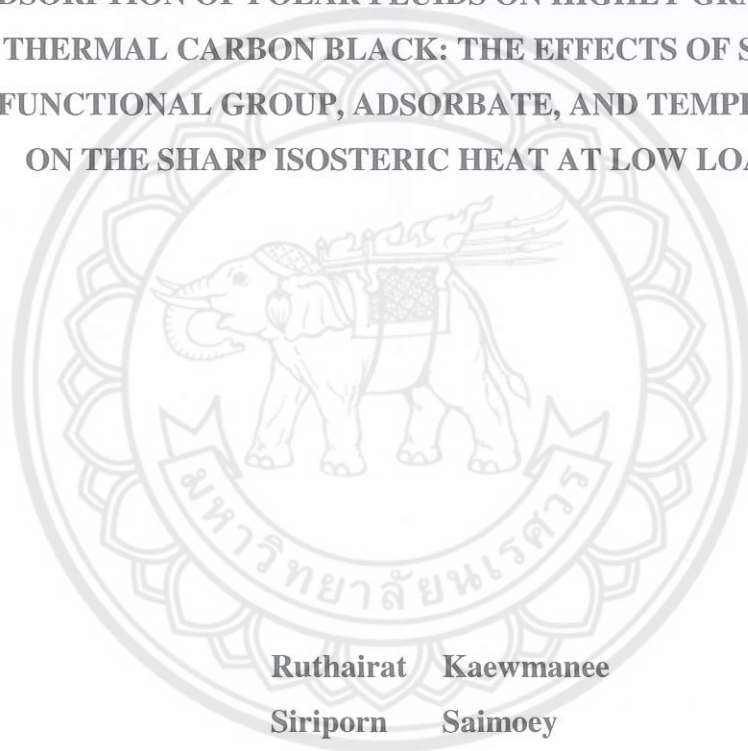 การดูดซับของของไหลที่มีขั้วบนพื้นผิวกราไฟท์ที่มีความบริสุทธิ์สูงโดยศึกษาผลกระทบของหมู่ฟังก์ชันบนพื้นผิว ชนิดตัวถูกดูดซับและอุณหภูมิต่อความร้อนของการดูดซับที่โหลดต่ำๆ

นางสาวฤทัยรัตน์   แก้วมณี   รหัส 54362913

นางสาวศิริพร   สายเหมย   รหัส 54362968

นางสาวสินีนาฏ   อินทรโยธา   รหัส 54362975

ADSORPTION OF POLAR FLUIDS ON HIGHLY GRAPHITIZED
THERMAL CARBON BLACK: THE EFFECTS OF SURFACE
FUNCTIONAL GROUP, ADSORBATE, AND TEMPERATURE
ON THE SHARP ISOSTERIC HEAT AT LOW LOADINGS

Ruthairat   Kaewmanee
Siriporn   Saimoey
Sineenach   Intarayotha

A Thesis Submitted in Partial Fulfillment of the Requirements for the

Bachelor Degree in Chemical Engineering

Naresuan University

Academic Year 2014

ใบรับรองปริญญานิพนธ์

ชื่อหัวข้อโครงงาน	การดูดซับของของไหลที่มีขั้วบนพื้นผิวกราไฟท์ที่มีความบริสุทธิ์สูงโดยศึกษาผลกระทบของหมู่ฟังก์ชันบนพื้นผิว ชนิดตัวถูกดูดซับและอุณหภูมิต่อความร้อนของการดูดซับที่โหลดต่ำๆ
ผู้ดำเนินโครงการ	นางสาวฤทัยรัตน์ แก้วมณี รหัส 54362913
	นางสาวศิริพร สายเหมย รหัส 54362968
	นางสาวสินีนาฏ อินทรโยธา รหัส 54362975
ที่ปรึกษาโครงงาน	ดร.นิคม กลมเกลี้ยง
สาขาวิชา	วิศวกรรมเคมี
ภาควิชา	วิศวกรรมอุตสาหการ
ปีการศึกษา	2557

....

    คณะวิศวกรรมศาสตร์ มหาวิทยาลัยนเรศวร อนุมัติให้ปริญญานิพนธ์ฉบับนี้เป็นส่วนหนึ่งของการศึกษาตามหลักสูตรวิศวกรรมศาสตรบัณฑิต สาขาวิชาวิศวกรรมเคมี

....ที่ปรึกษาโครงงาน
(ดร.นิคม กลมเกลี้ยง)

....กรรมการ
(รองศาสตราจารย์ ดร.สมร หิรัญประดิษฐกุล)

....กรรมการ
(ดร.ปณัฐพงศ์ บุญนวล)

....กรรมการ
(อาจารย์อาภาภรณ์ จันทร์ปิรักษ์)

ชื่อหัวข้อโครงงาน	การดูดซับของของไหลที่มีขั้วบนพื้นผิวกราไฟท์ที่มีความบริสุทธิ์สูงโดยศึกษาผลกระทบของหมู่ฟังก์ชันบนพื้นผิว ชนิดตัวถูกดูดซับและอุณหภูมิต่อความร้อนของการดูดซับที่โหลดต่ำๆ	
ผู้ดำเนินโครงการ	นางสาวฤทัยรัตน์ แก้วมณี	รหัส 54362913
	นางสาวศิริพร สายเหมย	รหัส 54362968
	นางสาวสินีนาฏ อินทรโยธา	รหัส 54362975
ที่ปรึกษาโครงงาน	ดร.นิคม กลมเกลี้ยง	
สาขาวิชา	วิศวกรรมเคมี	
ภาควิชา	วิศวกรรมอุตสาหการ	
ปีการศึกษา	2557	

บทคัดย่อ

วิทยานิพนธ์เล่มนี้ได้ทำการศึกษาไอโซเทอมของการดูดซับ (Adsorption isotherm) และพลังงานความร้อนของการดูดซับ (Isosteric heat) ในระดับไมโครของของไหลมีขั้วบนพื้นผิวกราไฟท์ที่มีความเป็นกราไฟท์สูงโดยใช้แบบจำลองแกรนด์ คาร์โนนิคอล มอลติ คาร์โล การลดลงอย่างรวดเร็วของค่าพลังงานความร้อนของการดูดซับสอดคล้องกับไอโซเทอมของการดูดซับซึ่งได้แสดงผลกระทบต่างๆที่ส่งผล เช่น ผลกระทบจากพื้นที่ผิวของหมู่ฟังก์ชัน ผลกระทบของตัวถูกดูดซับ (น้ำ และเมทานอล) และผลกระทบของอุณหภูมิ ในช่วงปริมาณของการดูดซับที่เกิดขึ้นจากแรงดึงดูดระหว่างของไหลกับพื้นที่ผิวที่มีหมู่ฟังก์ชันได้ปลดปล่อยค่าพลังงานความร้อนของการดูดซับออกมาในปริมาณสูงซึ่งสูงกว่าพลังงานความร้อนของการดูดซับของการประพฤติตัวเหมือนของเหลวจากนั้นการดูดซับก็จะลดลงเรื่อยๆจนถึงค่าพลังงานความร้อนของการดูดซับที่ต่ำที่สุดซึ่งน้อยกว่าค่าพลังงานความร้อนของการดูดซับที่ของไหลมีการประพฤติตัวเหมือนของเหลวที่ซึ่งโมเลกุลมีการรวมตัวกันเป็นกลุ่มที่แข็งแรงเมื่อแรงกระทำระหว่างของเหลวกับของไหล ที่โหลดสูงๆโมเลกุลจะมีการรวมตัวกันเป็นกลุ่มใหญ่ขึ้นจนถึงขอบเขตที่ค่าพลังงานของการดูดซับที่จะรับได้

....

ABSTRACT

This research studies microscopically the adsorption isotherms and isosteric heats of polar fluids on highly graphite surface. The sharp decrease of isosteric heat corresponding to its isotherm adsorbed is illustrated with the effect such as concentration of surface functional group, adsorbate such as water and methanol, and temperature. The initiated account for adsorption due to the strong fluid-surface functional group interaction releases a high isosteric which is higher than that of liquefaction. The further adsorption releases less and reaches the minimum isosteric heat which is extremely less than that of liquefaction where the molecules start to form a strong cluster. When the fluid-fluid interaction becomes dominated at higher loading the cluster becomes bigger, therefore the adsorbed heat reach the heat of liquefaction as liquid-like.
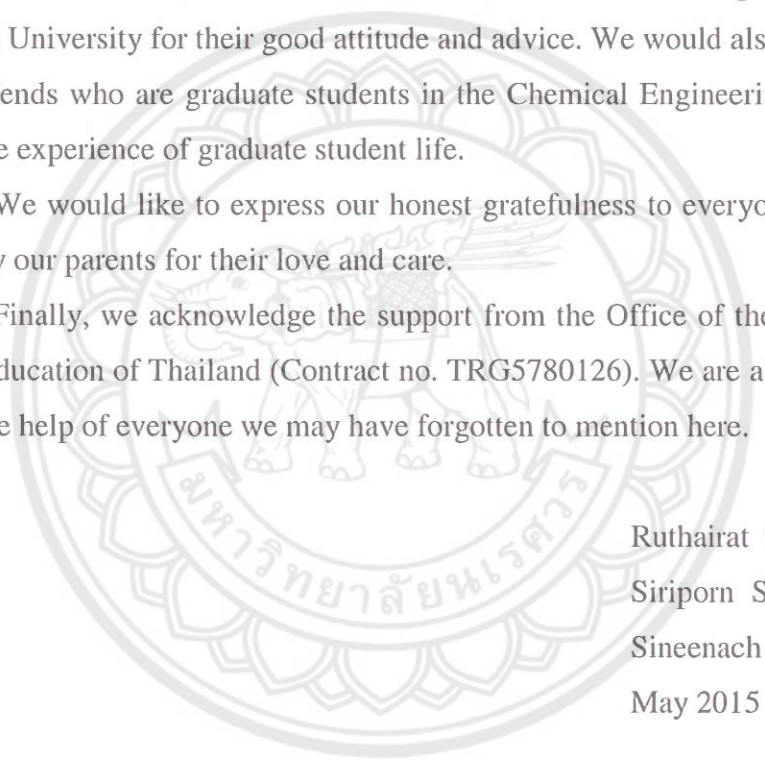
ACKNOWLEDGEMENTS

LIST OF CONTENTS

LIST OF CONTENTS (CONT.)

Page

LIST OF TABLES

Table **Page**

LIST OF FIGURES

LIST OF FIGURES (CONT.)

CHAPTER I

INTRODUCTION AND LITERATURE REVIEW

1.1 Significance of the problem

Adsorption is a simple technology to separate mixtures or purify wastewater [3-5]. Applications of liquid adsorption systems have been used such as organic removal from water or organic solvents, removal of contaminants with the color of organic substances, isolation of fermentation products, isolation from paraffin leave aromatic. Applications of gas adsorption systems have been used such as removal of water vapor from hydrocarbon gas, removal of sulfur from natural gas. The solvent was removed from the air and other gases and deodorization of air. Gravity happened in the adsorption process depends on the presence of polar or non-polar fluids and adsorbent.

Physical adsorption of polar fluids on graphitized thermal carbon black (GTCB) has been widely studied experimentally and theoretically [1, 2, 6-14]. Due to the fundamentals of adsorption of this adsorbate-adsorbent interaction are the basic step to better design of adsorption systems for polar fluids in pore whose walls are graphitic [15-17].

1.2 Literature reviews

Early experimental studies of adsorption of polar fluids such as water, methanol and ethanol on graphite surface were made by Kiselev and co-worker [1, 14], Pierce' s group [18] and Miura and Morimoto' s group [8, 19]. They measured adsorption isotherms with a volumetric apparatus and isosteric heats with a calorimetric. Their results play the role differed from that of non-polar adsorptions [12, 20]. Interestingly, Miura and Morimoto data showed the sharp decrease of isosteric heat at very low loadings. Recently, this was confirmed experimentally by Do's group [21], because initially, the strong interaction between polar molecule-strong active site which release adsorbed heat with a high value (higher than that of liquefaction) depending on the interaction of fluid-strong active site. Once the all

strong active sites is occupied and when the pressure is slightly increased the further molecules try to be adsorbed, to grow the cluster due to pressure is not high enough, resulting the system releases less adsorbed heat. When pressure is further increased the cluster can be formed the system releases more adsorbed heat due to the strong F-F interaction to reach the heat of liquefaction at higher loadings. However, the sharp decrease of isosteric heat could not be observed if the carbon black was not treated at temperature high enough. This is clearly done by Miura and Morimoto work. Miura and Morimoto studied water adsorption on graphite with the effect of treated temperature of adsorbent. The isosteric heat was decreased with increasing of treated temperature. The concentration of surface functional group at higher temperature treatment should be less than that of lower temperature treatment. It meant that the concentration of surface functional group play a role on this behavior. Due to the amount of active site affect directly to how strong the interaction between F-active site. There are several parameters that can influence on this interaction such as adsorbate, temperature. Together with computer simulation this can give detailed contributions of various interactions: fluid–fluid, fluid-basal plane and fluid-functional group.

In this research, we study microscopically using grand canonical Monte Carlo (GCMC) simulation on the sharp decrease of isosteric heat at low loadings. Polar fluids such as water and methanol are considered to figure out the effect of different strong polar fluid. Furthermore, the effect of temperature and concentration of surface functional group is investigated.

1.3 Research Objectives

The main aim of this research is to study the effects of the strength of hydrogen bonding on Graphitized Thermal Carbon Black by using grand canonical Monte Carlo simulation. This is achieved through the following specific objectives.

1. To study microscopically using grand canonical Monte Carlo (GCMC) simulation on the sharp decrease of isosteric heat at low loadings.

2. To study polar fluids such as water and methanol to figure out the effect of different strong polar fluid.

3. To study the effect of temperature and concentration of surface functional group.

1.4 Scope

The present research is focused on physical adsorption of polar fluids on graphitized thermal carbon black using Monte Carlo simulation. The study is separated into two main parts.

The first part is focused on the adsorption behaviors of polar fluids such as water, methanol and ethanol on graphitized thermal carbon black at ambient temperature. We study adsorption isotherms and isosteric heats at low loadings.

In the second part, adsorption behaviors of polar fluids on functionalized graphite surface are studied. We study the effects of concentration of surface functional group, adsorbate and temperature.

1.5 Outcomes

We can understand microscopically the adsorptions and isosteric heats of polar fluids such as water, methanol and ethanol on a highly graphite surface which is better to design the adsorption of polar fluids in graphitic pore. In this research can be used to study adsorption of mixtures for separation and purification involving water, methanol and ethanol.

CHAPTER II

THEORY AND METHODOLOGY

2.1 Fluid potential model

There are many different models of water have been proposed; they can be classified by the number of points used to define the model (Atoms plus dummy sites), whether the structure is rigid or flexible, and whether the model includes polarization effects. We believe that a good prediction of vapor-liquid equilibria (VLE) is a prerequisite for adsorption studies [22]. Therefore, we shall consider the TIP4P/2005 model [23] to represent with only dispersive and Coulombic forces. We use TraPPE model to describe methanol and ethanol [24, 25]. The molecular parameters of water, methanol, ethanol and surface phenol group are listed in Table 2.1 and polar fluids model is shown in Figures 2.1-2.3.
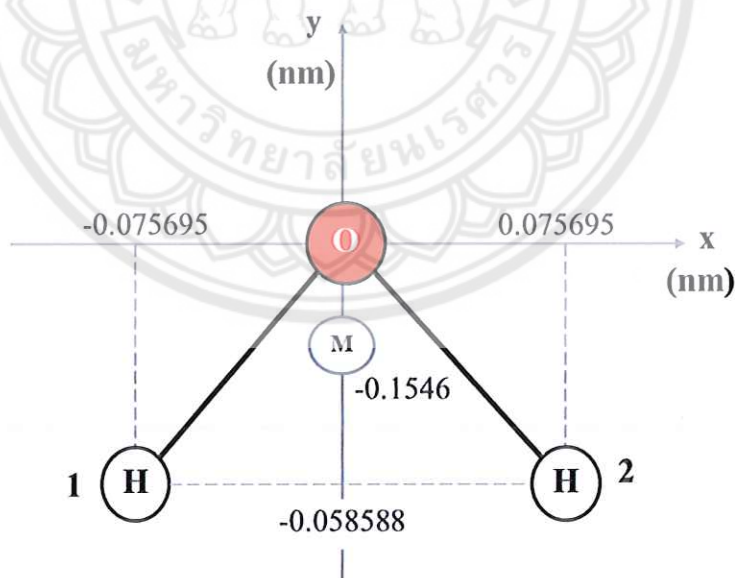
Figure 2.1 TIP4P/2005 of water.
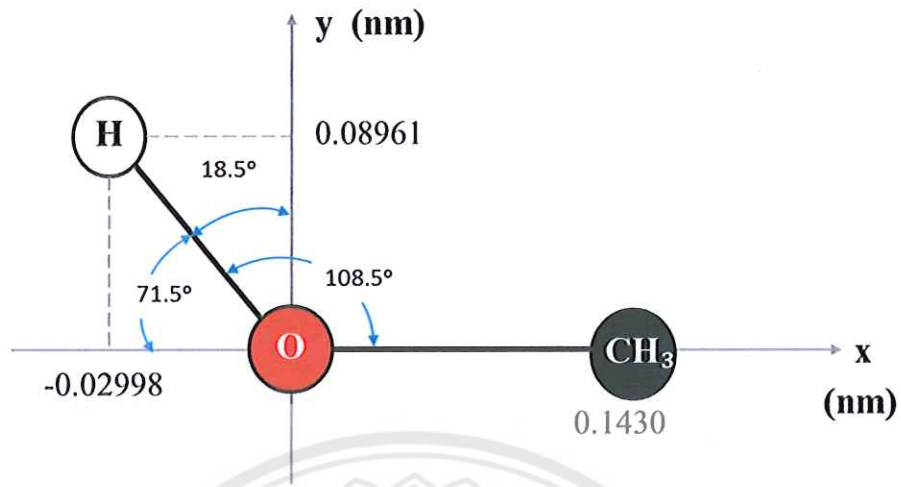
Figure 2.2 Methanol model.
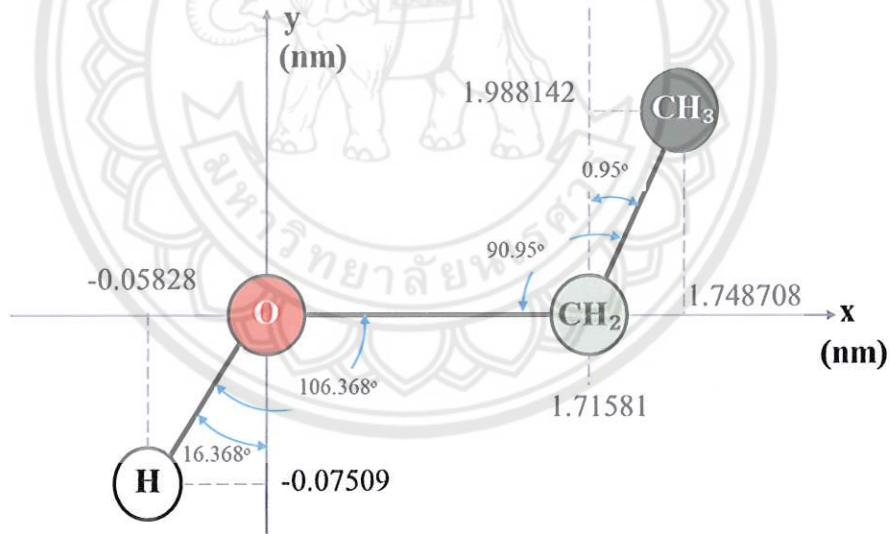
Figure 2.3 Ethanol model.

Table 2.1 Potential parameters for fluid and surface phenol group models.

Fluids/Functional group	x (nm)	y (nm)	z (nm)	σ (nm)	ε/k_B (K)	q (e)
Water						
O	0	0	0	0.31589	93.2	-
M	0	-0.01546	0	-	-	−1.1128
H(1)	-0.075695	-0.058588	0	-	-	+0.5564
H(2)	0.075695	-0.058588	0	-	-	+0.5564
Methanol						
CH₃	0.1430	0	0	0.375	98.0	0.265
O	0	0	0	0.302	93.0	-0.700
H	-0.02998	0.08961	0	-	-	0.435
Ethanol						
O	0	0	0	0.31496	85.053	-0.69711
CH₂	1.71581	0	0	0.34612	86.291	0.2556
CH₃	1.748708	1.988142	0	0.36072	120.15	-
H	-0.05828	-0.07509	0	-	-	0.44151
Surface phenol group						
Cₐ	0	0	0	-	-	0.2
O	0	0	0.1364	0.307	78.2	0.64
H	0	0.08992	0.17002	-	-	0.44

For a polyatomic molecule with M site centers, the potential energy of interaction between a site a on a molecule i with a site b on a molecule j can be calculated using the following LJ 12–6 equation:

$$U_{i,j}^{(a,b)} = \sum_{a=1}^{M}\sum_{b=1}^{M} 4\varepsilon_{i,j}^{(a,b)}\left[\left(\frac{\sigma_{i,j}^{(a,b)}}{r_{i,j}^{(a,b)}}\right)^{12} - \left(\frac{\sigma_{i,j}^{(a,b)}}{r_{i,j}^{(a,b)}}\right)^{6}\right] \tag{2.1}$$

where $r_{i,j}^{(a,b)}$ is the separation distance between the LJ site a on molecule i and the LJ site b on molecule j, $\sigma_{i,j}^{(a,b)}$ and $\varepsilon_{i,j}^{(a,b)}$ are the cross collision diameter and the cross well-depth of the interaction energy, respectively. The cross parameters, $\sigma_{i,j}^{(a,b)}$ and $\varepsilon_{i,j}^{(a,b)}$ can

be determined by the Lorentz–Berthelot mixing rules: $\sigma_{i,j}^{(a,b)} = (\sigma_{i,j}^{(a,a)} + \sigma_{i,j}^{(b,b)})/2$ and $\varepsilon_{i,j}^{(a,b)} = (\varepsilon_{i,j}^{(a,a)} \varepsilon_{i,j}^{(b,b)})^{1/2}$. The interaction energy due to the electrostatic force between a charge α on a molecule i and a charge β on a molecule j can be calculated from the Coulomb law of electrostatic interaction.

$$U_{q;i,j}^{(\alpha,\beta)} = \sum_{\alpha=1}^{M_q} \sum_{\beta=1}^{M_q} \frac{1}{4\pi\varepsilon_0} \frac{q_i^\alpha q_j^\beta}{r_{i,j}^{(\alpha,\beta)}} \tag{2.2}$$

where M_q is the number of charges on the molecule, ε_0 is the permittivity of free space [$\varepsilon_0 = 10^7/(4\pi c^2) = 8.8543 \times 10^{-12}$ $C^2J^{-1}m^{-1}$, c is the speed of light], $r_{i,j}^{(\alpha,\beta)}$ is the distance between two charges α and β on molecules i and j, respectively, q_i^α is the value of charge α on molecule i, and q_j^β is the value of charge β on molecule j. In the present work, for adsorption of adsorbate on surface comparison to experimental data, surface mediation is taken into account because of the surface influence on the interaction among adsorbed molecules close to the surface [1, 2].

2.2 Fluid-basal plane interaction energy

We have shown in our earlier work [26] that the graphite surface can be effectively modelled as a structure-less surface because the simulation results from this surface model are practically the same as those from the discrete atom model of the graphite surface. The potential energy between one adsorbate molecule and a graphite surface is calculated from the 10–4–3 Steele equation [27]:

$$U_{i,s} = \sum_{a=1}^{M} 4\pi\varepsilon_i^{(a,s)} \rho_s \left[\sigma_i^{(a,s)}\right]^2 \left[\frac{1}{5}\left(\frac{\sigma_i^{(a,s)}}{z_i^a}\right)^{10} - \frac{1}{2}\left(\frac{\sigma_i^{(a,s)}}{z_i^a}\right)^4 - \frac{\left[\sigma_i^{(a,s)}\right]^4}{6\Delta\left(z_i^a + 0.61\Delta\right)^3} \right] \tag{2.3}$$

where z_i^a is the distance of site a of molecule i from the graphite surface, $\varepsilon_i^{(a,s)}$ and $\sigma_i^{(a,s)}$ are the adsorptive-graphite interaction potential well-depth and intermolecular collision diameter respectively (Estimated with the Lorentz-Berthelot mixing rule),

ρ_s is the surface density (Taken as 38.2nm^{-2} in this work), and Δ is the spacing between the two adjacent graphite layer (0.3354nm). The molecular parameters for a carbon atom in the graphene layer are $\sigma_i^{(s)} = 3.4\text{Å}$ and $\varepsilon_i^{(s)}/k_B = 28K$.

Surface functional group
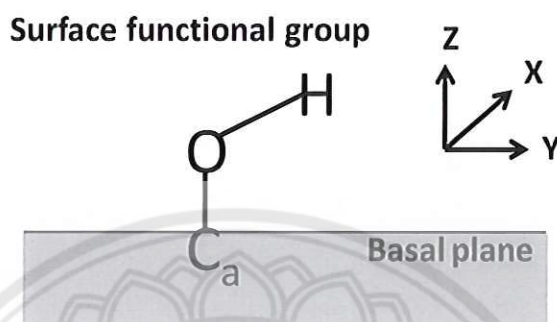
Figure 2.4 Side view of surface phenol group on the basal plane.

2.3 Surface functional group potential model

The strong active sites on the graphitized thermal carbon black are possible resulted from the procedure at high temperature due to the impurities of gas agent and the precursor itself. One of the strong active sites is surface functional group that is possibly formed at the edge of the graphene sheet or on the defected surface [28]. The surface functional groups such as carboxylic, phenol, and carbonyl can be found [8]. We model the highly GTCB by phenol group located on the graphite surface as shown in Figure 2.4. The concentrations of surface phenol group can be made by adding one molecule on the surface center with different surface area. The phenol group model is taken from the literature [8] where the LJ and Coulombic parameters are listed in Table 2.1.

2.4 Methodology

2.4.1 Grand canonical Monte Carlo simulation

For modelling an open surface, we used a slit pore wide enough to behave as two independent surfaces. The box length is more than 10 times the collision diameter, and the cut-off radius taken to be half of the box length. The standard Metropolis sampling scheme [29] was applied. The number of cycles for the equilibration and

statistics collection steps was 1×10^6 each. In each cycle, there are 1,000 moves of displacement (With rotation), and insertion (With rotation) and deletion with equal probability.

The average surface excess for an open surface was calculated from

$$\Gamma_{av} = \frac{\langle N \rangle - \rho_b V_{acc}}{2A} \tag{2.4}$$

where ρ_b is the bulk molecular density, A is surface area of one wall of the simulation box, V_{acc} is the accessible volume, and $\langle N \rangle$ is the ensemble average of the number of particles in the pore.

A thermodynamic quantity of interest that can be readily obtained from the GCMC is the isosteric heat. Using the fluctuation theory [30], it is calculated from [31]

$$q_T = q_{F-F} + q_{F-S} \tag{2.5}$$

$$q_{F-S} = q_{F-SBP} + q_{F-SFG} \tag{2.6}$$

$$q_T = \frac{\langle U \rangle \langle N \rangle - \langle UN \rangle}{\langle N^2 \rangle - \langle N \rangle \langle N \rangle} + k_B T \qquad \text{; total heat} \tag{2.7}$$

$$q_{F-F} = \frac{\langle U_{FF} \rangle \langle N \rangle - \langle U_{FF} N \rangle}{\langle N^2 \rangle - \langle N \rangle \langle N \rangle} + k_B T \qquad \text{; fluid-fluid} \tag{2.8}$$

$$q_{F-SBP} = \frac{\langle U_{F-SBP} \rangle \langle N \rangle - \langle U_{F-SBP} N \rangle}{\langle N^2 \rangle - \langle N \rangle \langle N \rangle} \qquad \text{; fluid-surface basal plane} \tag{2.9}$$

$$q_{F-SFG} = \frac{\langle U_{F-SFG} \rangle \langle N \rangle - \langle U_{F-SFG} N \rangle}{\langle N^2 \rangle - \langle N \rangle \langle N \rangle} \qquad \text{; fluid-surface functional group} \tag{2.10}$$

where $\langle \, \rangle$ is the ensemble average, N is the number of particles, and U is the configuration energy of the system. Where q is isosteric heat subscript, T is total heat, F-F is fluid-fluid interaction, F-SBP is fluid-surface basal plane, and F-SFG is fluid-surface functional group.

There are 3 Monte Carlo moves in grand canonical Monte Carlo (GCMC); (1) Insertion, (2) Deletion and (3) Displacement Move, shown in Figure 2.5.

(1) Insertion; A random position in the simulation box is selected to insert a particle. To accept the insertion the total energy of the system before and after move must be calculated.

(2) Deletion; A particle in the simulation box is selected randomly to delete. To accept the deletion the total energy of the system before and after move must be calculated.

(3) Displacement; A particle in the simulation box is selected randomly to displace. To accept the displacement move the total energy of the system before and after move must be calculated. If the system is stable ($U_{total}<0$ & $U_{new}<U_{old}$) we accept.
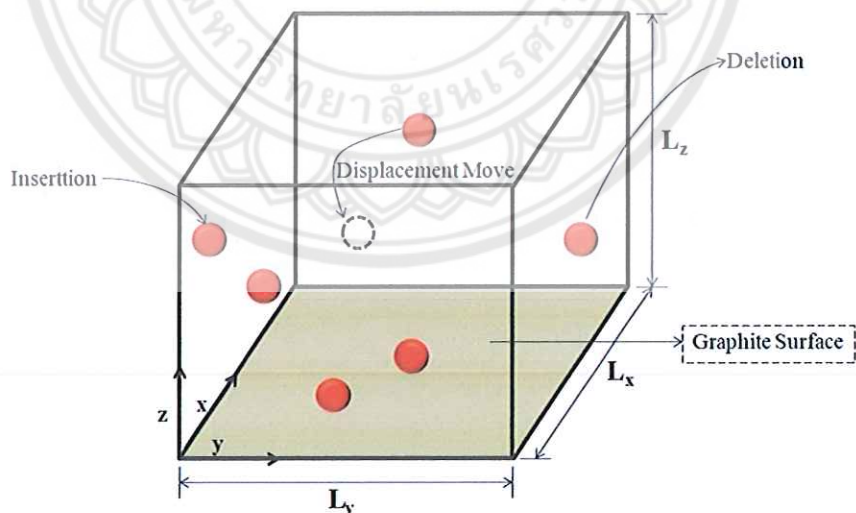
Figure 2.5 The grand canonical Monte Carlo (GCMC) simulation box.

CHAPTER III

RESULTS AND DISCUSSION

3.1 Water on highly GTCB

Adsorption on perfect graphite surface of water is widely studied in the literature, where reliable isotherms can be found [1]. Figures 3.1 and 3.2 show the adsorption isotherms and isosteric heats, respectively, at 293K of water obtained by our simulation with assumption of perfect graphite surface (Red line with unfilled circle) and experimental data from the literature [1]. The isotherm and heat curves are typical for water. Although these patterns have been thoroughly described in the literature, we shall explain briefly here for the purpose of comparison with the more interesting patterns of water. In the case for adsorption isotherms and isosteric heats on perfect graphite surface of water, methanol and ethanol is provided in the Appendix.
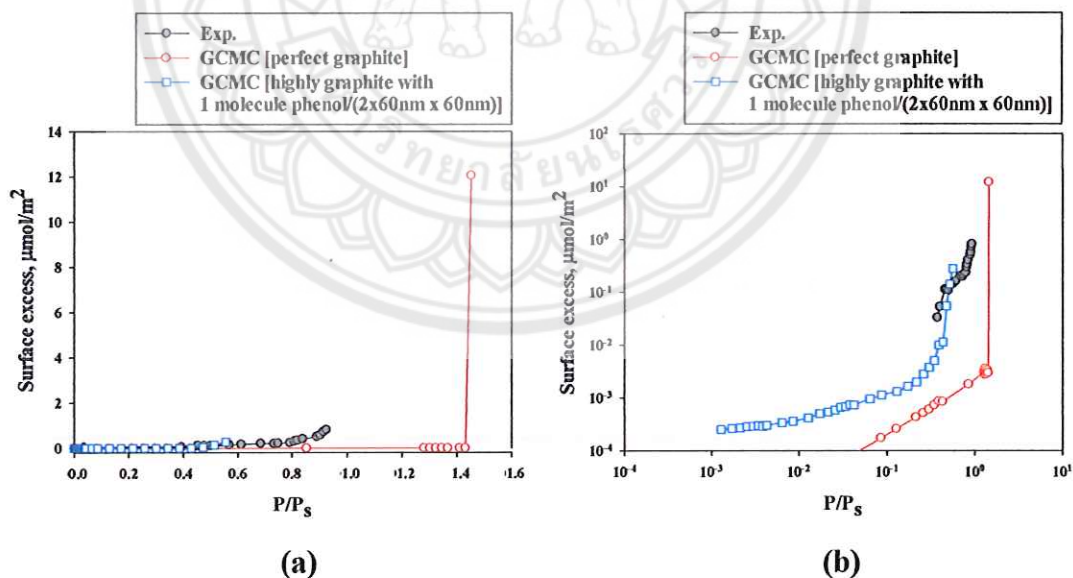
Figure 3.1 Adsorption isotherms of water on GTCB at 293 K; (a) linear scale and (b) logarithm scale. The experimental data are taken from the literature [1]. P_s is vapor pressure.
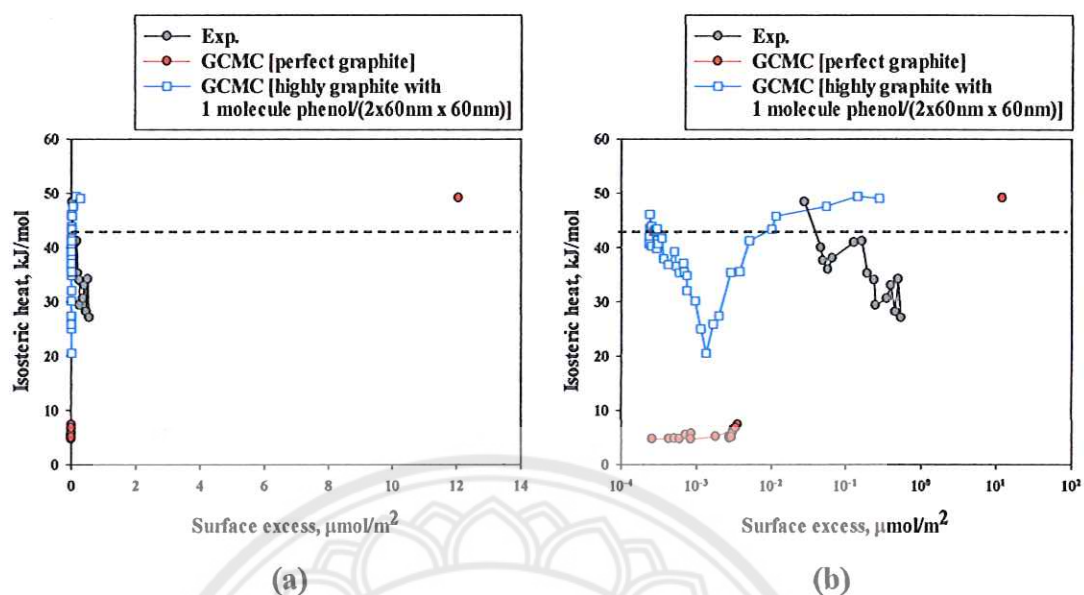
Figure 3.2 Isosteric heats of water on perfect graphite surface at 293 K; (a) linear scale and (b) logarithm scale. The experimental data are from the literature [1].

Water could not be adsorbed on the perfect graphite surface until the relative pressure of 1.42 due to water is a strong polar fluid while the perfect basal plane is non-polar site, therefore the interaction between water-perfect basal plane is so weak. However, the sharp adsorption is observed at relative pressure greater than 1.42 due to the confined space is assumed in the simulation. However, the experimental data showed the uptake of water which is slightly increased with pressure increase. Because the GTCB prepared from the experiment was not perfect graphite surface. There may be strong active sites at the edge of graphene layer or on the defect surface due to the high heat treatment. Therefore, we present in the Figures 3.1 and 3.2 (Line with square) the adsorption of water on the functionalized GTCB with concentration of 1 molecule phenol per (2 × 60 nm × 60 nm) at 293 K. It has been found that the water uptake as well as the isosteric heat on the functionalized surface yields the much improved data. Interestingly, particular at low loadings, the isosteric heat is sharply decreased which is in agreement with the experimental data from the literature.

As the loading is increased (Still less than the monolayer concentration), molecules, not only interact with the basal plane surface and the surface functional group, but also with the previously adsorbed molecules, resulting in the isosteric heat as the sum of the F-F interaction and a contribution from the F-basal plane and F-surface functional group interactions, which is proportional to the loading. There is a sharp decrease in the isosteric heat at very low loadings because molecules start to adsorb on the functional group that the system releases a high isosteric heat (Due to the strong F-functional group), then the system releases less when the functional group already occupied by a few adsorbate but cluster have not formed (Molecules just form and orientate themselves to interact with the functional group with a stable state) due to the pressure is low enough that polar fluid cluster cannot be formed. The isosteric heat is turned to increase due to the cluster at higher pressures can be performed. After many cluster and/or layers have been formed on the surface, the isosteric heat approaches the heat of liquefaction because the adsorbates in the higher loadings are liquid-like. The feature will be described microscopically in the next section.

3.2 Effect of concentration of surface functional group

There was a measurement of water adsorption on highly graphite surface at 298 K by Morimoto [8]. The highly graphite surface was treated at different temperatures 25, 700 and 1000°C. The isosteric heats were decreased at low loadings with treated temperature increase as shown in Figure 3.3a. This is interesting that the effect of strong active site plays the role to the sharp decrease of isosteric heat at low loadings. Together with Figure 3.3b we show isosteric heat of water on the functionalized graphite surface at 298 K with different concentrations of surface functional group from 1 molecule phenol per (2×16 nm $\times 16$ nm) to 1 molecule phenol per (2×60 nm $\times 60$ nm) for comparison with Morimoto data. It found that at concentration value high enough (1 molecule phenol per (2×16 nm $\times 16$ nm)) the sharp decrease of heat lower than that of liquefaction (Dash line) cannot be found. When the concentration is slightly decreased the sharp decrease lower than that of the dash line can be observed. We shall explain the mechanism by using the contribution of F-F, F-basal plane, and F-surface function group interactions as shown in Figure 3.4.
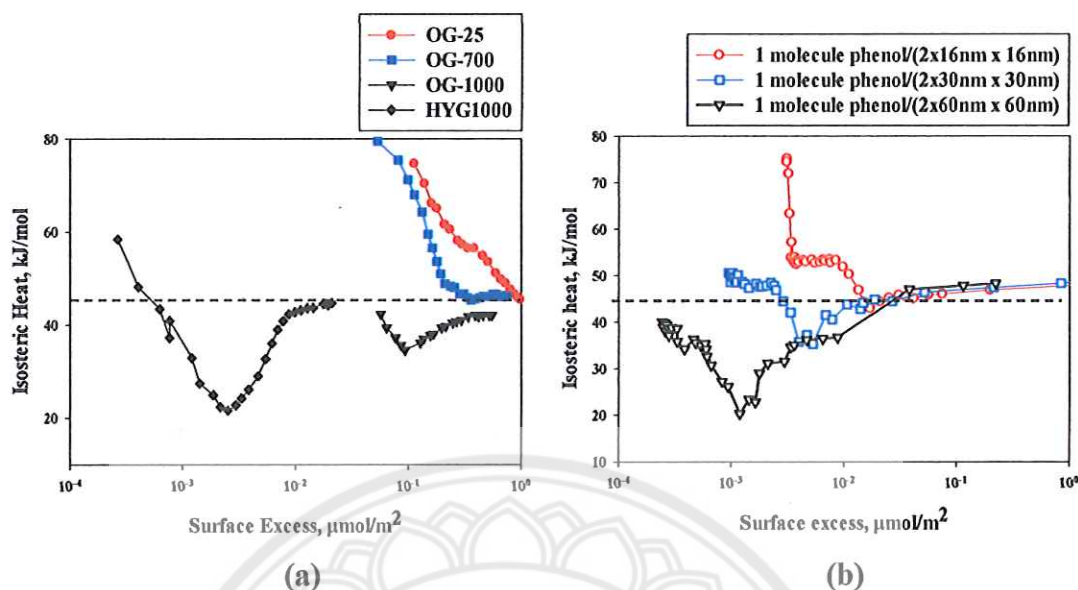
Figure 3.3 **Isosteric heat of water adsorption on highly graphite surface at 298 K; (a) data from the literature [8, 32] and (b) results from GCMC with different concentrations of surface functional group.**

The heat of water adsorption shows high heat release at the initial stage of adsorption, which is due to the direct interaction between water molecule and functional groups by hydrogen bonding because this interaction is much greater than the interaction between water and the basal plane (See Figure 3.4). Further increase in pressure leads to the continuing growth of water clusters because the water-water interaction (Via hydrogen bonding) is greater than water-basal plane interaction. When this cluster is very small the interaction in adsorption is between water and about two neighboring water molecules on the boundary of the cluster. This leads to a minimum in the heat curve. As loading is further increased the cluster merges with neighboring clusters, and water will interact with increasing number of neighbors, giving rise to an increase in the heat. Finally the isosteric heat approaches the heat of liquefaction because large water clusters has the bulk water-like behavior.
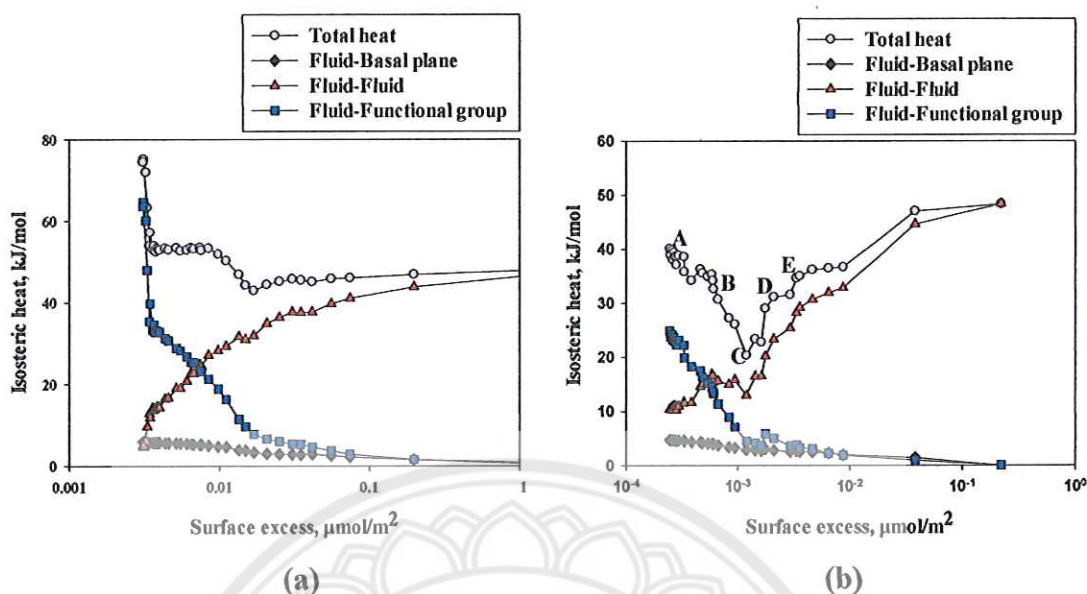
Figure 3.4 Isosteric heats of water on highly GTCB at 298 K with the concentration of surface functional group of (a) 1 molecule phenol per (2 × 16 nm × 16 nm) and (b) 1 molecule phenol per (2 × 60 nm × 60 nm).

This behavior of water adsorption at low loadings is because of the following order of interactions: water-functional group>>water–water>>water-basal plane, therefore, the mechanism of water adsorption essentially follows a sequential mechanism: (1) adsorption of water on the functional group, followed by (2) water cluster growth due to the water-water interaction.

We can now summarize the mechanism of water adsorption graphically in Figure 3.5, and the following steps occur in sequence:

Point A

Direct interaction of water molecule and the functional group is formed. The system releases the high heat value.

Point B

Few molecule is adsorbed.
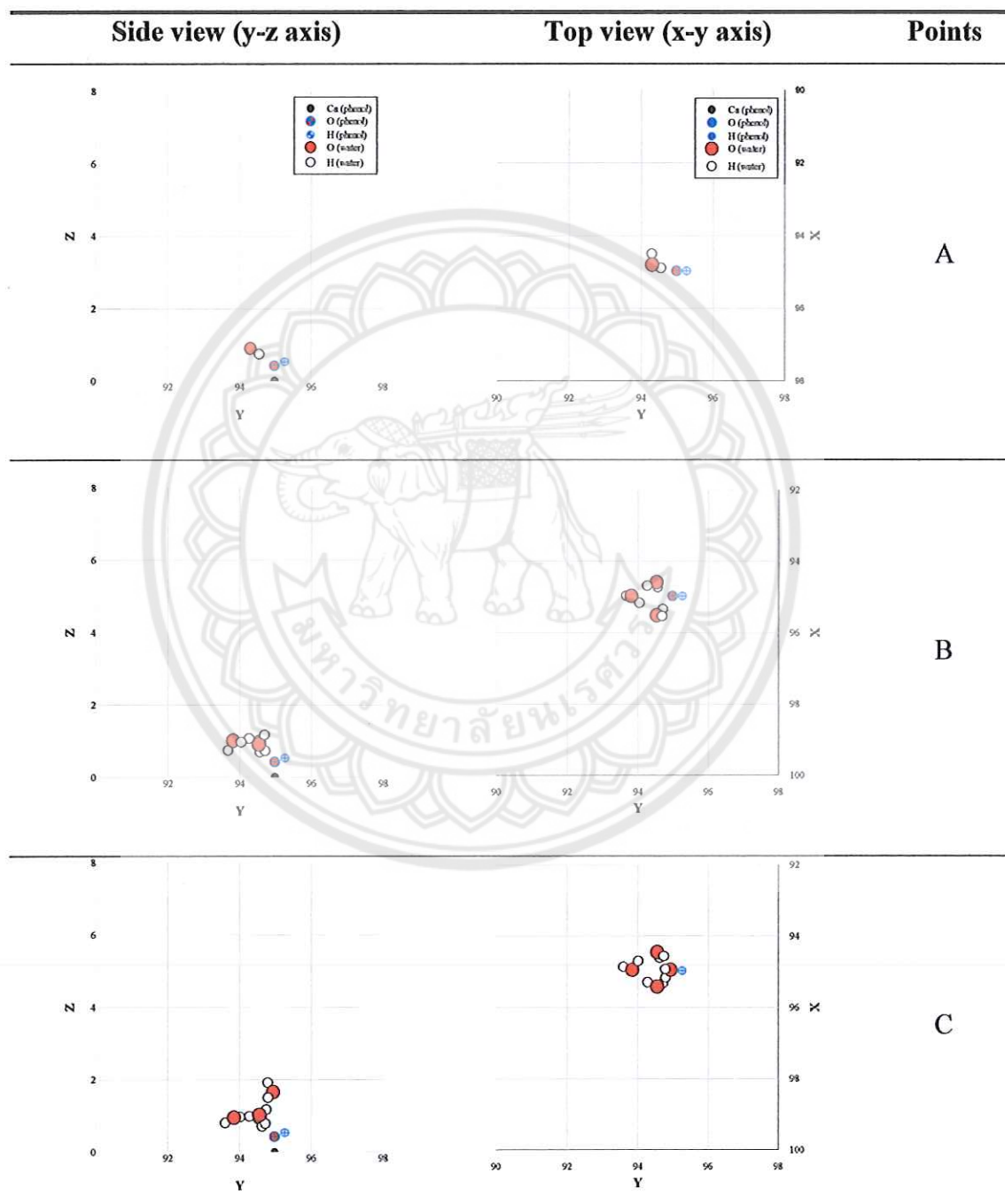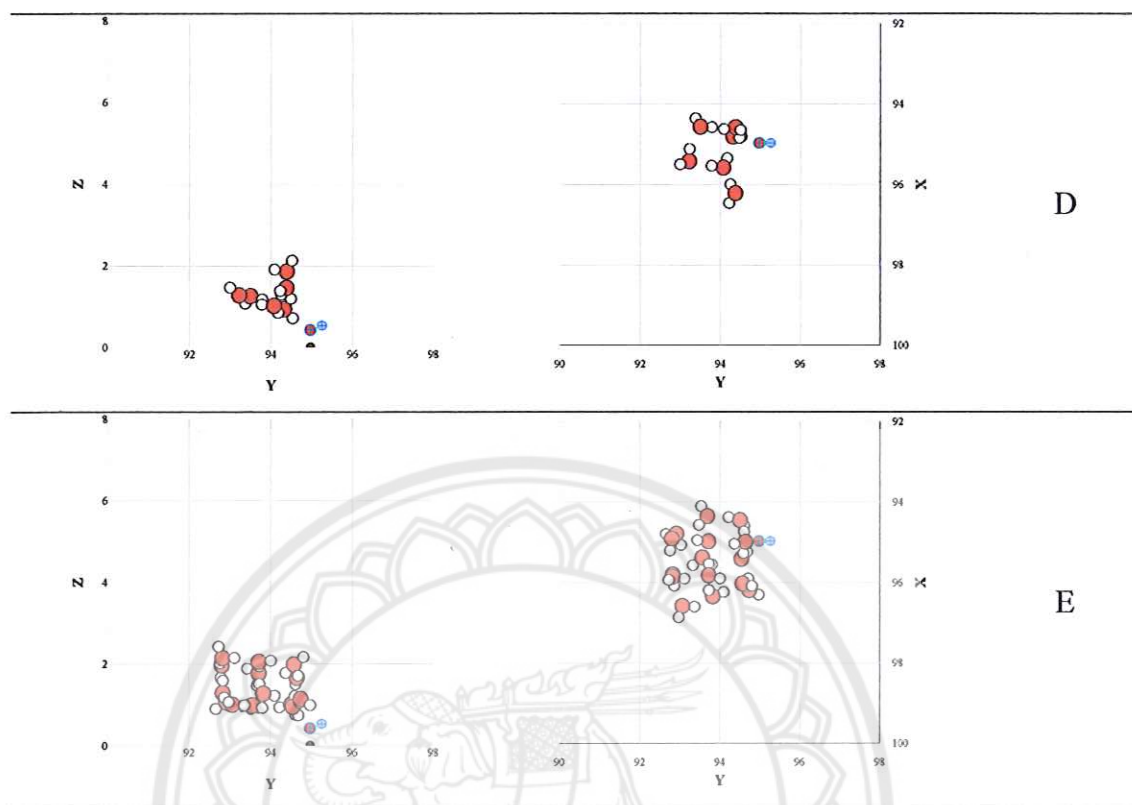
Point C

Growth of water on the boundary of small water cluster; the heat of adsorption is minimized.

Points D and E

Adsorption of water on either the "wavy" boundaries of clusters or in between neighboring clusters; the heat is about the same as the heat of liquefaction.

Side view (y-z axis)	Top view (x-y axis)	Points
		A
		B
		C

Figure 3.5 The process adsorption of water on the highly GTCB at 298 K; the highly GTCB has the concentration of surface functional group of 1 molecule phenol per (2 × 60 nm × 60 nm). Points A-E are indicated in Figure 3.4b.

3.3 Effect of adsorbate

Figure 3.6 shows methanol adsorption on the highly GTCB at 298 K with different concentrations of surface functional group with the experimental data from the literature. The observation is similar to that of water, when the concentration is decreased the minimum heat is decreased. However, at a given concentration of surface functional group, the isosteric heat of methanol is decreased more than that of water as shown in Figure 3.7a. This is due to water-functional group is stronger than methanol-functional group. What we have seen the contributions that lead the F-functional group interaction, influence the sharp decrease of isosteric heat at low loadings; one is concentration of surface functional group and other one is kind of adsorbate.

(a)

(b)
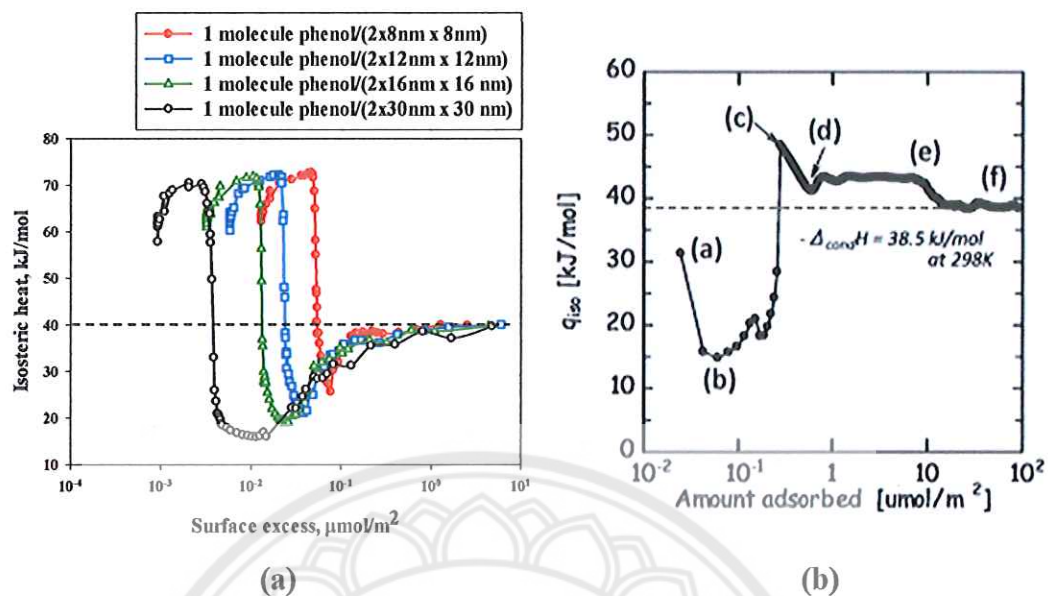
Figure 3.6 Isosteric heats of methanol on highly GTCB at 298 K with the different concentrations of surface functional group. The experimental data are taken from the literature [21].

(a)

(b)
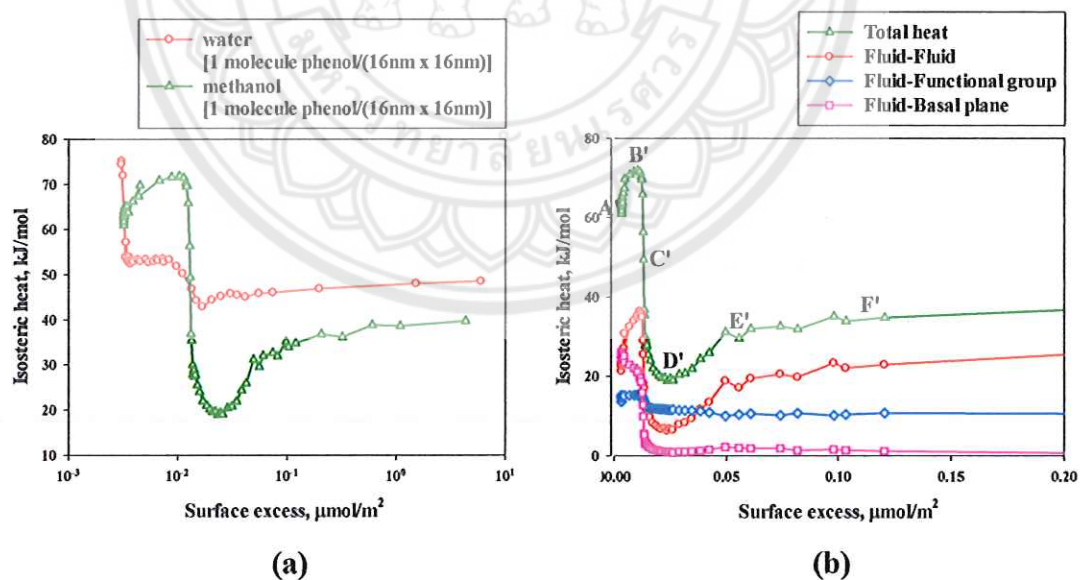
Figure 3.7 Isosteric heats of polar fluids on highly GTCB at 298 K with the concentration of surface functional group of 1 molecule phenol per (2 × 16 nm × 16 nm). (a) Total isosteric heats of water and methanol; (b) F-F, F-functional group, and F-basal plane of methanol.

Figure 3.7b, the initial adsorption accounts for the interaction of one molecule methanol with the functional groups, the isosteric heat is higher than the dash line (Point A'), followed by adsorption of few methanol molecules around this complex, the adsorbed heat slightly increased (Point B'). At Point C' methanol-basal plane is started higher than methanol-functional group where the adsorption releases the less heat than previous point. At Point D', the adsorption reach the minimum heat about 20 kJ/mol where a strong cluster is initiated. At Points E' and F', the heat released is purely by the intermolecular interaction of methanol (Fluid–fluid interaction). As loadings greater than Point C' where methanol-basal plane greater than methanol-functional group, methanol begins to spill over onto the basal plane because of the methyl group of methanol. However, water case the water molecules do not spill over onto the basal plane due to water-basal plane is so weak (See Figure 3.4).
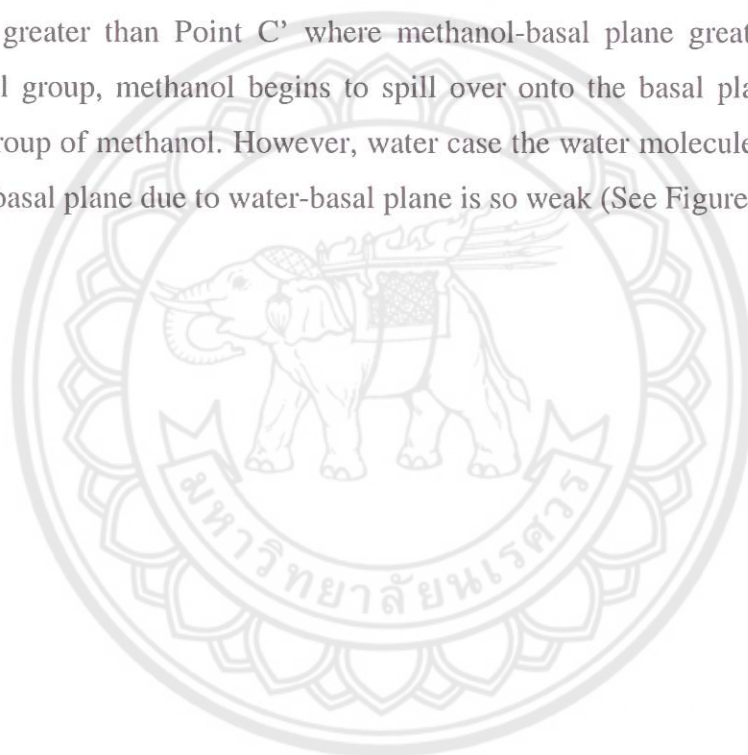
We now summarized the mechanism of methanol adsorption in Figure 3.8.

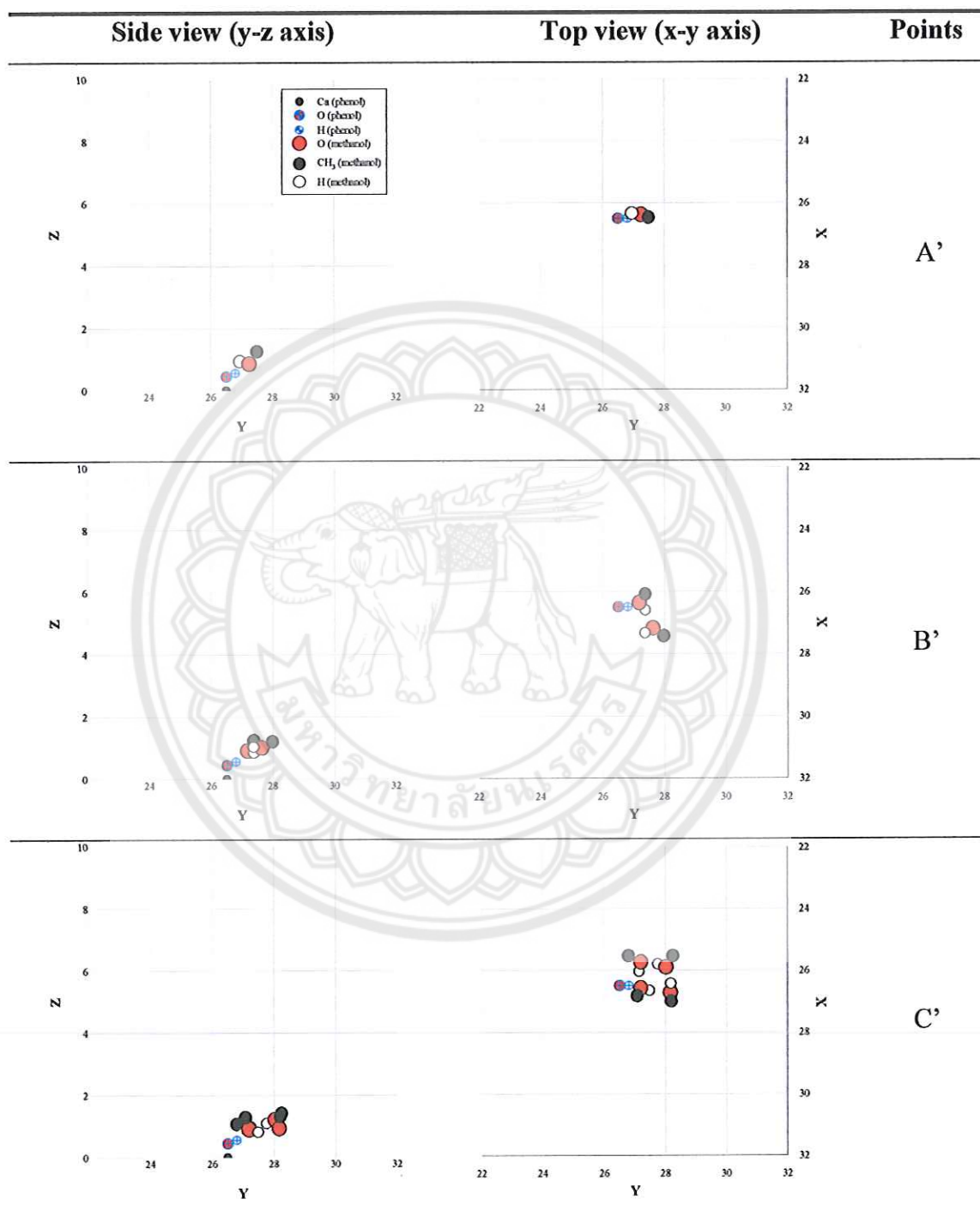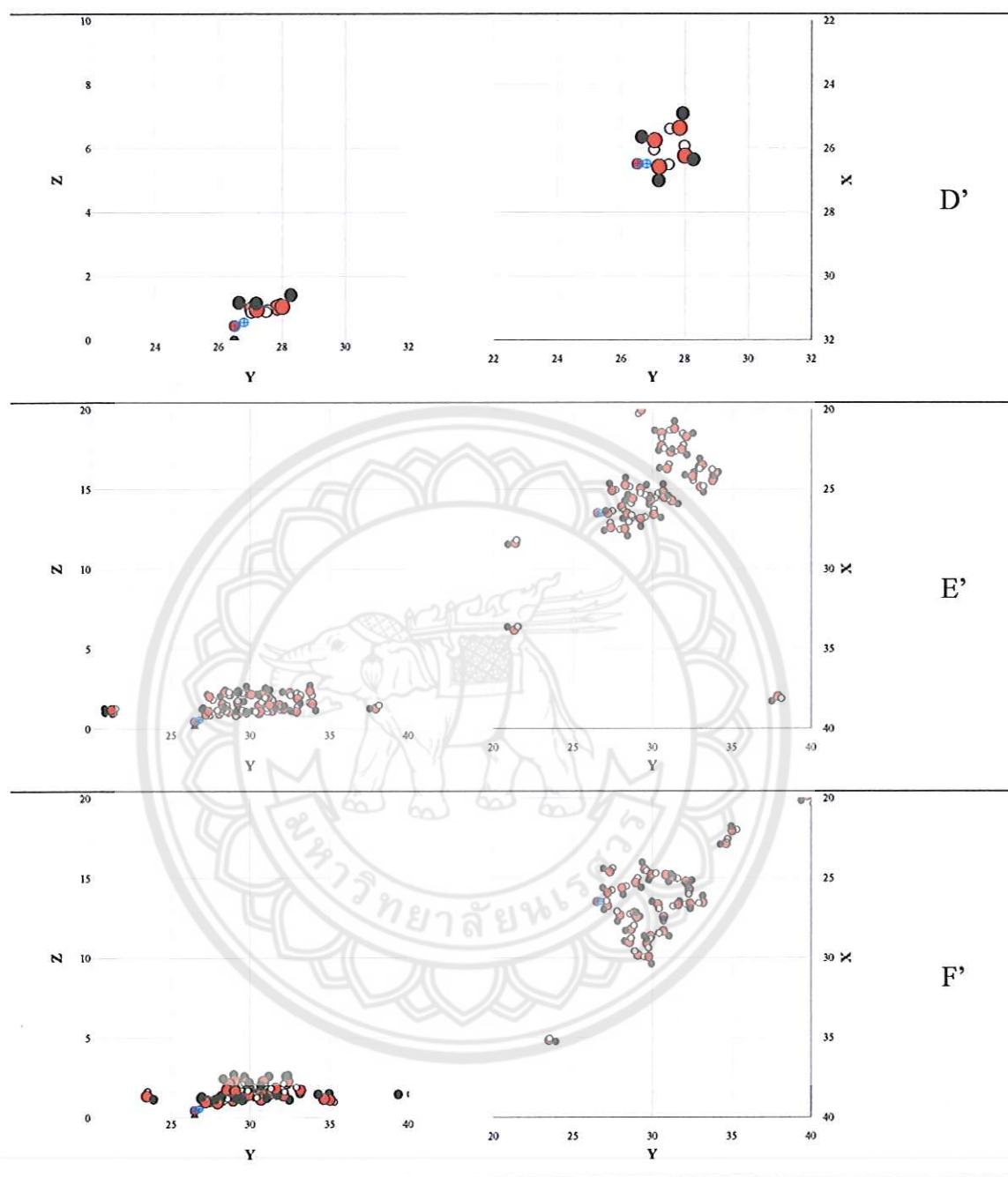| Side view (y-z axis)	Top view (x-y axis)	Points
		A'
		B'
		C'

Figure 3.8 Snapshots of methanol on highly GTCB at 298 K with the concentration of surface functional group of 1 molecule phenol per (2 × 16 nm × 16 nm). Points A' to F' are indicated in Figure 3.7b.

CHAPTER IV

CONCLUSIONS

4.1 Conclusions

We have presented the difference in the isosteric heats of water and methanol adsorptions on a highly graphitized carbon black. The pattern of the isosteric heat versus loading shed great insight into how molecules interact with the surface. The isosteric heats water and methanol exhibit a complex pattern with respect to loading, but it is a fingerprint in showing the relative interplay between the various interactions, fluid–fluid, fluid-basal plane and fluid-functional group. The isosteric heats of methanol and water adsorption were high at the initial stage of adsorption because molecules favor to adsorb on functional group due to the stronger fluid-functional group interaction than F-F or F-basal plane interactions. Once a cluster has been formed on the functional group, subsequent behaviors of the heat curves of methanol and water are different. For methanol the heat increases rapidly because the 2D-clusters start to spread on the graphite surface, and finally the heat is the same as the heat of liquefaction. However, for water, the heat increases with loading and finally approaches the heat of liquefaction because water does not adsorb on the graphite surface, i.e. the water molecules adsorb on either the "wavy" boundaries of clusters or in between neighboring clusters.

4.2 Recommendation

This study is the fundamentals of adsorption. Thus, we recommend that researcher who interested in gas separation involving polar fluids such as water, methanol and ethanol can be able to start from our work. In addition, this can be applied for water treatment using adsorption.

REFERENCES

REFERENCES

1. Avgul, N.N., Berezin, G.I., Kiselev, A.V., Lygina, I.A., The adsorption and heat of adsorption of normal alcohols on graphitized carbon black. Bulletin of the Academy of Sciences of the USSR, Division of chemical science, 1961. 10(2): p. 186-193.

2. Nguyen, V.T., Do, D.D., Nicholson, D., tagiello, J., Effects of Temperature on Adsorption of Methanol on Graphitized Thermal Carbon Black: A Computer Simulation and Experimental Study. The Journal of Physical Chemistry C, 2011. 115(32): p. 16142-16149.

3. Olanipekun, O., Oyefusi,A., Neelgund, G.M., Oki,A., Adsorption of lead over graphite oxide. Spectrochim Acta A Mol Biomol Spectrosc, 2014. 118: p. 857-60.

4. Viard, B., Pihan, F., Promeyrat,S., Pihan, J.C., Integrated assessment of heavy metal (Pb, Zn, Cd) highway pollution: bioaccumulation in soil, Graminaceae and land snails. Chemosphere, 2004. 55(10): p. 1349-59.

5. El-Sheikh, A.H., Effect of oxidation of activated carbon on its enrichment efficiency of metal ions: comparison with oxidized and non-oxidized multi-walled carbon nanotubes. Talanta, 2008. 75(1): p. 127-34.

6. Birkett, G.R. and D.D. Do, Simulation study of methanol and ethanol adsorption on graphitized carbon black. Molecular Simulation, 2006. 32(10-11): p. 887-899.

7. Birkett, G.R. and D.D. Do, Simulation Study of Water Adsorption on Carbon Black: The Effect of Graphite Water Interaction Strength. The Journal of Physical Chemistry C, 2007. 111(15): p. 5735-5742.

8. Morimoto, T. and K. Miura, Adsorption sites for water on graphite. 1. Effect of high-temperature treatment of sample. Langmuir, 1985. 1(6): p. 658-662.

9. Zeng, Y., Prasetyo, Luisa, Nguyen, Van T., Horikawa, Toshihide, Do, D.D., Nicholson, D., Characterization of oxygen functional groups on carbon surfaces with water and methanol adsorption. Carbon, 2015. 81: p. 447-457.

10. Morimoto, T. and K. Miura, Adsorption sites for water on graphite. 2. Effect of autoclave treatment of sample. Langmuir, 1986. 2(1): p. 43-46.

11. Nguyen, V.T., Horikawa, T., D.D.Do, Nicholson, D., Water as a potential molecular probe for functional groups on carbon surfaces. Carbon, 2014. 67(0): p. 72-78.

12. Nguyen, V.T., Horikawa, T., D.D.Do, Nichol son, D., On the relative strength of adsorption of gases on carbon surfaces with functional groups: fluid–fluid, fluid–graphite and fluid–functional group interactions. Carbon, 2013. 61(0): p. 551-557.

13. Nguyen, V.T., D.D. Do, and D. Nicholson, A new molecular model for water adsorption on graphitized carbon black. Carbon, 2014. 66(0): p. 629-636.

14. Belyakov, L.D., A.V. Kiselev, and N.V. Kovaleva, Gas-Chromotographic Determination of Isotherms and Heats of Adsorption of Water, Benzene and Methanol Vapours on Graphitised Carbon Black. Russian Journal of Physical Chemistry, 1968. 42(9): p. 1204-1208.

15. Wang, Y., Nguyen, Phuong T.M., Sakao, N., Horikawa, T. D, D.D.Do, Morishige, K., Nicholson, D., Characterization of a New Solid Having Graphitic Hexagonal Pores with a GCMC Technique. Journal of Physical Chemistry C, 2011. 115(27): p. 13361-13372.

16. Morishige, K., Layer-by-Layer Freezing of Kr Confined in Hexagonal Pores with Crystalline Carbon Walls. Journal of Physical Chemistry C, 2011. 115(24): p. 12158-12162.

17. Morishige, K. and N. Tateishi, Adsorption hysteresis in ink-bottle pore. Journal of Chemical Physics, 2003. 119(4): p. 2301-2306.

18. Pierce, C. and R.N. Smith, The Heats of Adsorption. III. Methanol on Carbon. The Journal of Physical and Colloid Chemistry, 1950. 54(3): p. 354-364.

19. Miura, K. and T. Morimoto, Adsorption sites for water on graphite. 5. Effect of hydrogen-treatment of graphite. Langmuir, 1991. 7(2): p. 374-379.

20. Do, D.D., Johnathan Tan, S.L., Zeng, Yonghong, Fam, Chunyan Nguyen, Van T., Horikawa, Toshihide, Nicholson, D., The interplay between molecular layering and clustering in adsorption of gases on graphitized thermal carbon black – Spill-over phenomenon and the important role of strong sites. Journal of Colloid and Interface Science, 2015. 446(0): p. 98-113.

21. Horikawa, T., Zeng, Yog hong, Do, D.D., Sotowa, Ken0Lchire Alcantara Avila, Jesus Raafael., On the isosteric heat of adsorption of non-polar and polar fluids on highly graphitized carbon black. Journal of Colloid and Interface Science, 2015. 439(0): p. 1-6.

22. Jorge, M., C. Schumacher, and N.A. Seaton, Simulation Study of the Effect of the Chemical Heterogeneity of Activated Carbon on Water Adsorption. Langmuir, 2002. 18(24): p. 9296-9306.

23. Abascal, J.L.F. and C. Vega, A general purpose model for the condensed phases of water: TIP4P/2005. The Journal of Chemical Physics, 2005. 123(23): p. 234505.

24. Chen, B., J.J. Potoff, and J.I. Siepmann, Monte Carlo Calculations for Alcohols and Their Mixtures with Alkanes. Transferable Potentials for Phase Equilibria. 5. United-Atom Description of Primary, Secondary, and Tertiary Alcohols. The Journal of Physical Chemistry B, 2001. 105(15): p. 3093-3104.

25. Schnabel, T., J. Vrabec, and H. Hasse, Henry's law constants of methane, nitrogen, oxygen and carbon dioxide in ethanol from 273 to 498 K: Prediction from molecular simulation. Fluid Phase Equilibria, 2005. 233(2): p. 134-143.

26. Klomkliang, N., Do, D.D., Nicholson, D., Tangsathitkulchai, C. wongkoblap, A., Multilayer adsorption of benzene on graphitised thermal carbon black—The importance of quadrupole and explicit hydrogen in the potential model. Chemical Engineering Science, 2012. 69(1): p. 472-482.

27. Steele, W.A., Phyical interaction of gases with crystalling solids.1. Gas-solid energies and properties of isolated adsorbed atoms. Surface Science, 1973. 36(1): p. 317-352.

28. Tarasevich, Y.I. and E.V. Aksenenko, Interaction of water, methanol and benzene molecules with hydrophilic centres at a partially oxidised model graphite surface. Colloids and Surfaces A: Physicochemical and Engineering Aspects, 2003. 215(1-3): p. 285-291.

29. Allen, M.P. and T.P. Tildesley, Computer Simulation of Liquids. Japanese Journal of Applied Physics Part 2-Letters, 1987. 35(3B): p. L405-L407.

30. Ahmaruzzaman, M., Adsorption of phenolic compounds on low-cost adsorbents: A review. Advances in Colloid and Interface Science, 2008. 143(1-2): p. 48-67.

31.   Araujo, R.S., Azevedo, D.C.S., cavalcants Jr., C.L., Jimenez-Lopzz, A., Rudriguez-Castelon, E., Adsorption of polycyclic aromatic hydrocarbons (PAHs) from isooctane solutions by mesoporous molecular sieves: Influence of the surface acidity. Microporous and Mesoporous Materials, 2008. 108(1-3): p. 213-222.

32.   Miura, K. and T. Morimoto, Adsorption sites for water on graphite. 3. Effect of oxidation treatment of sample. Langmuir, 1986. 2(6): p. 824-828.
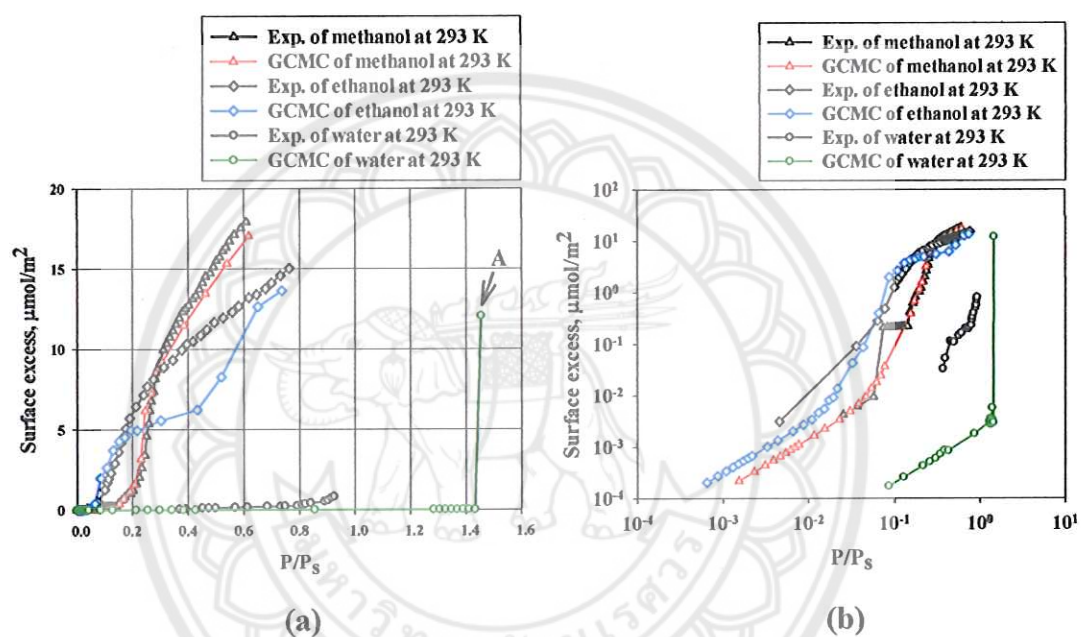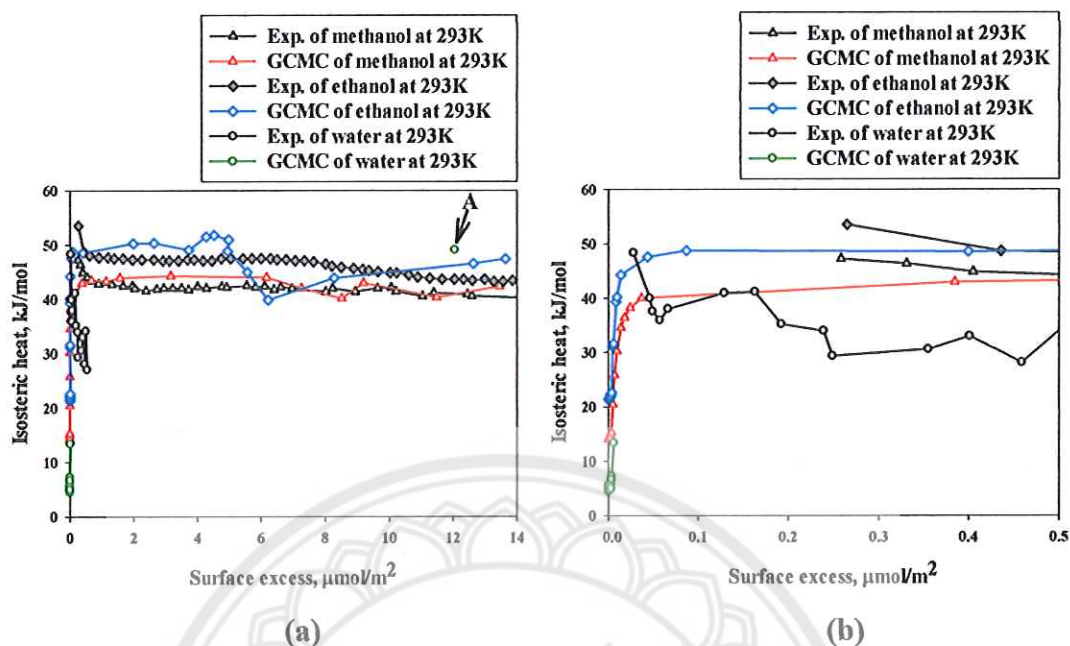
APPENNDIXES

Water, methanol and ethanol adsorptions on perfect graphite surface

Water, methanol and ethanol adsorptions and isosteric heats graphite surface at 293 K obtained by GCMC and experimental data is show in Figures A1 and A2, respectively. It has found that the simulation results is quite in agreement with the experimental data exception of water adsorption. Due to the adsorbent prepared from experiment was not that a perfect graphite surface.

Figure A1 Adsorption isotherms of water, methanol and ethanol on GTCB at 293 K; (a) linear scale and (b) logarithm scale. The experimental data are taken from the literature [1, 2].

Figure A2 Isosteric heats of water, methanol and ethanol on **perfect graphite** surface at 293 K; (a) at high loadings and (b) at low **loadings. The** experimental data are from the literature [1, 2].

The isosteric heat of water form experimental data at low loadings is lower than that of the liquefaction that the isosteric heat from GCMC with perfect graphite surface assumption could not described. Because the total isosteric heat from the perfect surface is contributed from F-F and F-Solid basal plane interactions as shown in Figure A3. We provide more evidence when the polar fluids like methanol and ethanol adsorb on a preface graphite surface by snapshot in Figure A4.
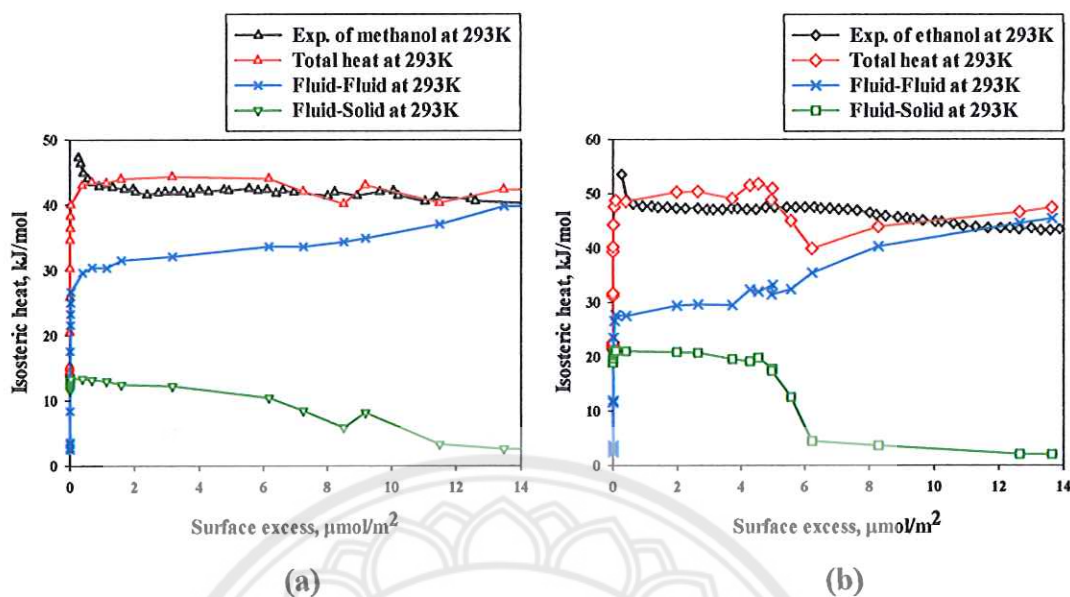
Figure A3 F-F and F-S isosteric heats of methanol and ethanol on perfect graphite surface at 293 K. The experimental data are taken from the literature [1].
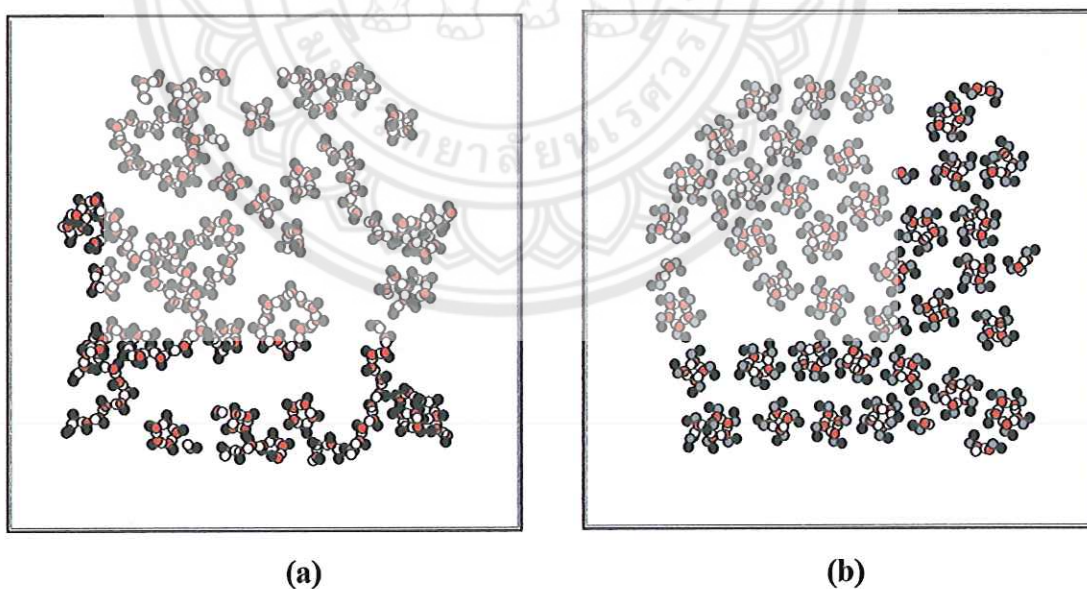
Figure A4 Top view of (a) methanol and (b) ethanol on perfect graphite surface at 293 K.

BIOGRAPHY

BIOGRAPHY

Name –Surname	Ruthairat Kaewmanee
Date of Birth	February 2, 1993
Place of Birth	Phrae, Thailand
Address	1/4,Padaeng, Amphor Mueang, Phrae, Thailand. 54000

Education Background

2014   B. Eng. (Chemical Engineering), Naresuan University, Thailand

Name –Surname	Siriporn Saimoey
Date of Birth	January 3, 1993
Place of Birth	Lampang, Thailand
Address	106/1, Lomrad, Amphor Thoen, Lampang, Thailand. 52160

Education Background

2014   B. Eng. (Chemical Engineering), Naresuan University, Thailand

Name –Surname	Sineenach Intarayotha
Date of Birth	December 12, 1991
Place of Birth	Surat Thani, Thailand
Address	94, Takanon, Amphor Khiri Ratnikhom, Surat Thani, Thailand. 84180

Education Background

2014   B. Eng. (Chemical Engineering), Naresuan University, Thailand